Heat capacity effect on ethanol preignition in a shock tube

Minh Bau Luong[1], Miguel Figueroa-Labastida[1], Efstathios-Al. Tingas[1], Aliou Sow[1],

Francisco E. Hernández Pérez[1], Jihad Badra[2], Aamir Farooq[1], Hong G. Im[1]

[1]Clean Combustion Research Center, King Abdullah University of Science and Technology,

Thuwal 23955-6900, Saudi Arabia

[2]Fuel Technology Division, R&DC, Saudi Aramco, Dhahran, 31311, Saudi Arabia

1 Introduction

Preignition is an undesired phenomenon that has been observed in different devices such as internal combustion engines and shock tubes [1-9]. In these devices, preignition is typically initiated by uncontrolled ignition sources such as hot spots and oil droplets. In a recent experimental shock-tube study, the ignition delay time measurement of mixtures with 5% ethanol and 30% O_2, having either Ar or N_2 as bath gas, showed a high uncertainty due to unexpected preignition phenomena [1]. The authors also found that under the same temperature and pressure conditions after the reflected shock wave, the Argon-containing mixtures are more prone to preignite than those containing N_2 and also have a shorter ignition delay time. Without preignition, the homogenous ignition delay times of these mixture are nearly the same. The observed preignition phenomenon seems to link with on the fuel and oxidizer concentration and/or properties of the mixture, such as thermal diffusivity and laminar flame thickness [1].

Preignition is typically linked to the minimum ignition energy (MIE) [2]. MIE dictates a minimum amount of energy that is required to achieve a successful ignition kernel formation. MIE is characterized by the flame thickness, mixture density, and heat capacity. Since Ar has a considerably smaller heat capacity than N_2, it is suggested that heat capacity may be a key factor in the preignition propensity and different behaviors observed in the shock tube experiments of Figueroa-Labastida et al. [1]. The main objective of the present study is to investigate the effect of heat capacity on preignition development by varying the strength of an imposed ignition source which acts as a hot spot. In the following sections, the configuration and conditions under study are described, the results are presented and discussed, and conclusions are drawn.

2 Initial conditions

Correspondence to: minhbau.luong@kaust.edu.sa

One-dimensional (1-D) direct numerical simulations (DNS) are performed to study the hot spots that may appear in shock tubes. The hot spots may stem from a bifurcating shock wave that results in inhomogeneity in the mixtures. The ethanol reaction mechanism developed by Lu and co-authors [9] is adopted in this work.

The physical parameters of the four selected mixtures which exhibited the preignition formation are listed in Table 1. Note that the mass of the four tested mixtures in the shock tube experiments are nearly the same, the difference in their mass lies within 5%. The homogeneous ignition delays, τ_{ig}, of the four mixtures are plotted in Fig. 1 showing that all the cases also have nearly identical τ_{ig} despite the differences in composition and equivalence ratio, ϕ.

Cases	ϕ	Composition (mole %)
1	1.0	5% Ethanol - 15% O_2 - 80% Ar
2	1.0	5% Ethanol -15% O_2 - 80% N_2
3	0.5	5% Ethanol -30% O_2 - 65% Ar
4	0.5	5% Ethanol - 30% O_2 - 65% N_2

Table 1. Physical parameters of the four mixtures, chosen as in [1], with the pressure and temperature after the reflected shockwave being, respectively, P_5 of 2 bar, and T_5 of 900 K, 1000 K, 1100K, and 1200 K.

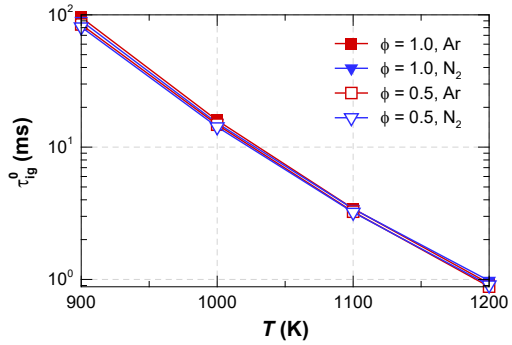

Figure 1. Homogeneous zero-dimensional (0-D) ignition delay time of the mixtures as a function of temperature.

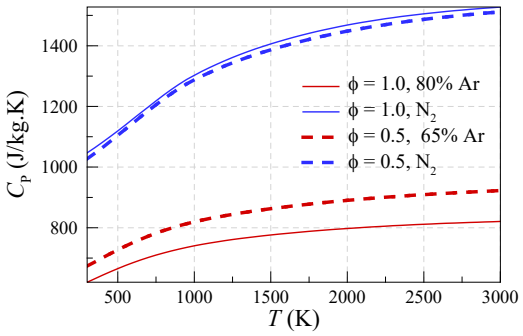

Figure 2. Heat capacity of the mixtures as a function of temperature.

As shown in Fig. 2, the Ar mixtures have lower heat capacities compared with those of the N_2 ones. It is expected that for the same amount of mass of ethanol/O_2/bath gas added to the shock tube and the identical initial conditions after the reflected shock wave (T_5 and P_5), if there exist hot spots, the local temperature of Argon-containing mixtures will increase more than that of the N_2 ones. This expectation is confirmed in the

next section by imposing different ignition sources. To this end, an ignition source term is added to the energy equation, which acts as a hot spot. The ignition source term for the 1-D simulations is defined as follows:

$$q_{ig} = \frac{E_{ig}}{r_{ig} t_{ig}} f(t),$$

$$f(t) = \frac{1}{a\sqrt{\pi}} \exp\left[-\frac{\left(t / t_{ig}\right)^2}{2a^2} \right]$$

where q_{ig} is the ignition source term and a = 0.125. E_{ig}, r_{ig}, and t_{ig} denote the total ignition energy, ignition kernel radius, and the duration of the ignition source. The values r_{ig} of 0.5 mm and t_{ig} of 0.1 ms are fixed while varying E_{ig}. Note that the same ignition energy strength is added to the four mixtures for each test suite of varying T_5 or E_{ig}.

3 Results and discussion

The effect of the heat capacity on the ignition delay time of the ethanol mixtures is examined by changing the bath gas, being either Ar or N_2. Different ignition source strengths are then varied to elucidate the response of τ_{ig} to the change in E_{ig} for four different mixtures. First, 0-D simulations are carried out, which are then followed by the representative selected 1-D simulations.

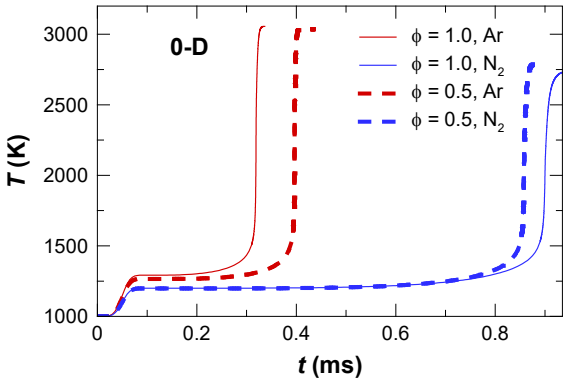

Figure 3. Representative temporal evolution of temperature for four different mixtures with the same imposed ignition-source strength from 0-dimensional (0-D) simulations.

Figure 3 shows representative 0-D simulation results for T_5 of 1000 K with q_{ig} = 1E-4 J/s. As seen in Fig. 3, for the same q_{ig}, the cases with Ar show a higher temperature increment as compared with the N_2 cases, which is about 80 K. This amount of temperature has a pronounced effect on the ignition delay difference between the mixtures with the two bath gases being used. The ignition delays of the Ar cases are more than two times shorter than those of the N_2 cases. Note that this effect is significantly amplified in the 0-D simulations when contrasted with the corresponding 1-D cases because there is no heat diffusion. This point is confirmed when comparing the 0-D and 1-D solutions plotted in Fig. 3 and Fig. 4, respectively, corresponding to the same applied ignition energy density. Figure 4 shows the consistent trend of ignition delay advancements between Ar cases and N_2 that was revealed by the 0-D simulations. However, the ignition delays associated with the 1-D cases are closer to the experimental results. Consistent with the magnitude of heat capacity shown in Fig. 2, the ignition delay time of four mixtures shown in Fig. 3 is in

the same order that τ_{ig} of N_2 case with $\phi = 0.5$ has a shorter than the N_2 case with $\phi = 1.0$ while τ_{ig} of Ar case with $\phi = 0.5$ has a longer than the Ar case with phi = 1.0.

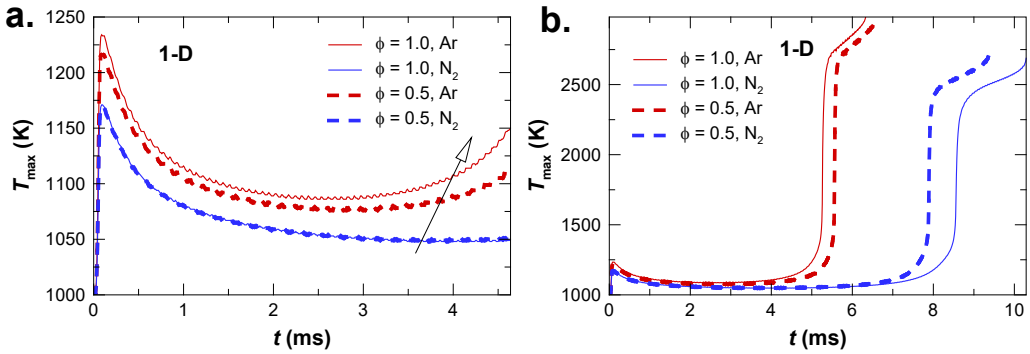

Figure 4. The temporal evolution of the maximum temperature from 1-dimensional (1-D) simulations.

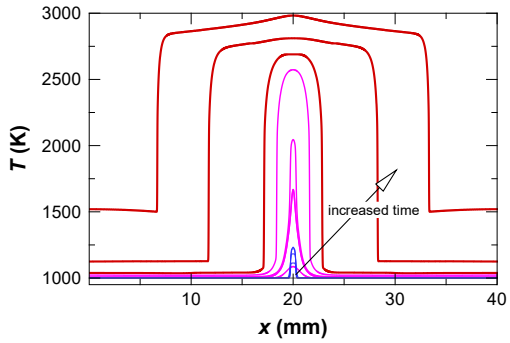

Figure 5. Temporal evolution of temperature for Case 1. The blue lines show the hot-spot induction period, the pink lines show the transition period of the ignition kernel formation, and the red lines show the main combustion event.

The time evolution of the peak temperature for the 1-D simulations is plotted in Fig. 4. It is seen that the Ar cases have a higher temperature increment than the N_2 cases after the mixture is heated up by the ignition source, about 60 K (see Fig. 4a). After the ignition-source induction period, the maximum temperature drops quickly due to the heat diffusion (see Fig. 5, blue-to-pink transition lines). Since the thermal diffusivities of the four mixtures are nearly identical (not shown here), the rate of the maximum temperature decrease of the mixtures is almost the same. As such, the amount of temperature difference by the ignition source still remains during the transition period to the hot ignition. By performing computational singular perturbation (CSP) analysis, we found that even a small difference in the temperature increment significantly facilitates the H_2O_2 decomposition reaction via $H_2O_2 + M \rightarrow OH + OH + M$, which is consistent with the findings in [10-12]. As a result, the mixtures containing Ar arrive at the ignition point much earlier than the ones containing N_2, as shown in Fig. 3 and Fig. 4b.

The sensitivity of the ignition delay times to various E_{ig} at different temperatures (T_5) is systematically evaluated and the results are plotted in Fig. 6 for the ignition delay time and Fig. 7 for the derivative of the ignition delay time with respect to E_{ig}. It is shown that τ_{ig} exponentially decreases with increasing magnitude of E_{ig} regardless of the bath gases being either Ar or N_2. However, the Ar cases exhibit a higher degree of sensitivity to E_{ig}, which translates into much smaller τ_{ig} than the N_2 cases under the same condition. This qualitatively substantiates the experimental observations [1].

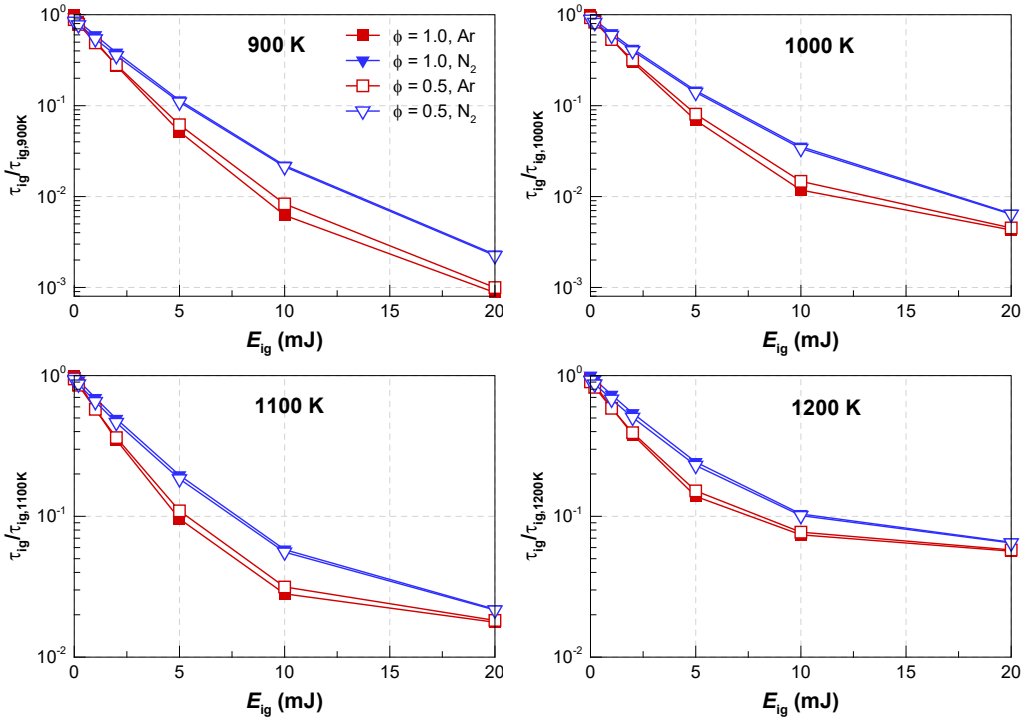

Figure 6. Homogeneous ignition delay time as a function of the imposed ignition energy, normalized by its 0-D ignition delay shown in Fig. 1 in which no E_{ig} is introduced.

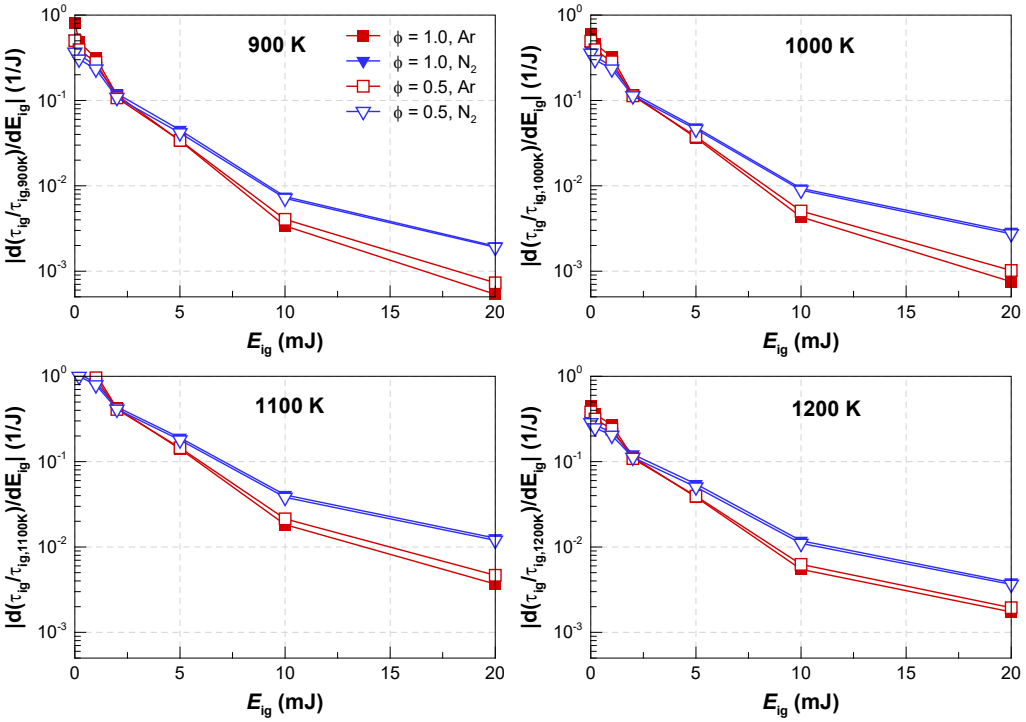

Figure 7. Sensitivity of the homogeneous ignition delay time with respect to the imposed ignition energy at four different temperatures of 900 K, 1000 K, 1100 K, and 1200 K.

4 Conclusion

Four different ethanol mixtures with bath gas being either Ar or N_2 were examined to identify the root cause of the preignition observed in a recent experimental study on a shock tube [1]. A hot spot was simulated by adding an ignition source to the energy equation. The ignition delay sensitivity of the ethanol mixtures with respect to the ignition source strength was parametrically investigated. It was found that the heat capacity difference between Ar and N_2 is the main reason for the higher preignition propensity of the Ar cases. Besides, a small difference in temperature increment can have a pronounced effect on accelerating the H_2O_2 decomposition reaction, $H_2O_2 + M \rightarrow OH + OH + M$, which in turn significantly shortens the ignition delay time of the mixtures containing Ar, when compared with the corresponding N_2 ones.

Acknowledgement

This work was sponsored by Saudi Aramco and competitive research funding from King Abdullah University of Science and Technology. This research used the resources of the KAUST Supercomputing Laboratory (KSL).

References

[1] M. Figueroa-Labastida, J. Badra, AM. Elbaz, A. Farooq, Shock tube studies of ethanol preignition, Combust. Flame 198 (2018) 176–185
[2] G.T. Kalghatgi, D. Bradley, Pre-ignition and 'super-knock' in turbo-charged spark-ignition engines, Int. J. Eng. Res. 13 (2012) 399–414.
[3] Bradley, D., Morley, C., Gu, X. J., and Emerson, D. R., "Amplified pressure waves during autoignition: relevance to CAI engines," SAE 2002-01-2868.
[4] E.M. Chapman, V.S. Costanzo, A literature review of abnormal ignition by fuel and lubricant derivatives, SAE Int. J. Eng. 9 (2015) 107–142.
[5] T. Javed, J. Badra, M. Jaasim, E. Es-Sebbar, M.F. Labastida, S.H. Chung, H.G. Im, A. Farooq, Shock tube ignition delay data affected by localized ignition phenomena, Comb. Sci. Tech. 189 (2017) 1138–1161.
[6] D.F. Davidson, R.K. Hanson, Interpreting shock tube ignition data, Int. J. Chem. Kinet. 36 (2004) 510–523.
[7] S.M. Walton, X. He, B.T. Zigler, M.S. Wooldridge, A. Atreya, An experimental investigation of iso-octane ignition phenomena, Combust. Flame 150 (2007) 246–262.
[8] Z. Wang, Y. Qi, X. He, J. Wang, S. Shuai, C.K. Law, Analysis of pre-ignition to super-knock: Hotspot-induced deflagration to detonation, Fuel 144 (2015) 222–227.
[9] Ali, M. J. M., Luong, M. B., Sow, A., Perez, F. H., and Im, H., "Probabilistic Approach to Predict Abnormal Combustion in Spark Ignition Engines," SAE 2018–01–1722
[9] A. Bhagatwala, J.H. Chen, T.F. Lu, Direct numerical simulations of HCCI/SACI with ethanol, Combust. Flame, 161 (2014) 1826-1841.
[10] Luong, M. B., Yu, G. H., Chung, S. H., and Yoo, C. S., Ignition of a lean PRF/air mixture under RCCI/SCCI conditions: *A comparative DNS study*," Proc. Combust. Inst. 36 (2017) 3623–3631.
[11] M. B. Luong, G. H. Yu, S. H. Chung, C. S. Yoo, Ignition of a lean PRF/air mixture under RCCI/SCCI conditions: *Chemical aspects*, Proc. Combust. Inst. 36 (2017) 3587–3596.
[12] Westbrook, Chemical kinetics of hydrocarbon ignition in practical combustion systems, Proc. Combust. Inst. 28 (2000) 1563–1577.